

# Kinetics of RNA Degradation by Specific Base Catalysis of Transesterification Involving the 2'-Hydroxyl Group

Yingfu Li and Ronald R. Breaker\*

Contribution from the Department of Molecular, Cellular and Developmental Biology, Yale University, PO Box 208103, New Haven, Connecticut 06520-8103

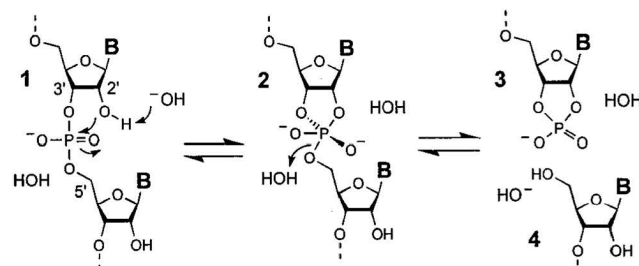
Received February 24, 1999

**Abstract:** A detailed understanding of the susceptibility of RNA phosphodiester to specific base-catalyzed cleavage is necessary to approximate the stability of RNA under various conditions. In addition, quantifying the rate enhancements that can be produced exclusively by this common cleavage mechanism is needed to fully interpret the mechanisms employed by ribonucleases and by RNA-cleaving ribozymes. Chimeric DNA/RNA oligonucleotides were used to examine the rates of hydroxide-dependent degradation of RNA phosphodiester under reaction conditions that simulate those of biological systems. Under neutral or alkaline pH conditions, the dominant pathway for RNA degradation is an internal phosphoester transfer reaction that is promoted by specific base catalysis. As expected, increasing the concentration of hydroxide ion, increasing the concentration of divalent magnesium, or raising the temperature accelerates strand scission. In most instances, the identities of the nucleotide bases that flank the target RNA linkage have a negligible effect on the  $pK_a$  of the nucleophilic 2'-hydroxyl group, and only have a minor effect on the maximum rate constant for the transesterification reaction. Under representative physiological conditions, specific base catalysis of RNA cleavage generates a maximum rate enhancement of  $\sim 100\,000$ -fold over the background rate of RNA transesterification. The kinetic parameters reported herein provide theoretical limits for the stability of RNA polymers and for the proficiency of RNA-cleaving enzymes and enzyme mimics that exclusively employ a mechanism of general base catalysis.

## Introduction

Ribonucleic acids perform critical functions in modern biological systems that range from information storage and transfer to structure formation and catalysis. Polymers of RNA are most commonly composed of the four standard ribonucleotides (G, A, U, and C) which are joined via 3',5'-phosphodiester linkages (Scheme 1, 1). The stability of RNA toward chemical and enzymatic degradation plays a central role in the biological function of this polymer. One of the greatest risks to the molecular integrity of RNA under conditions that approximate those found inside cells (near neutral pH and the presence of alkali metals and alkali-earth metals) is the inherent chemical instability of its RNA phosphodiester bonds. The close proximity of the adjacent 2'-hydroxyl group to the phosphorus center of each internucleotide linkage permits facile transesterification to occur, particularly under strongly acidic or strongly basic conditions.<sup>1</sup> Both acid-catalyzed and base-catalyzed reactions proceed via an  $S_N2$  mechanism wherein the 2' oxygen attacks the adjacent phosphorus center. It is largely the protonation state of the 2' oxygen that dictates the rate at which each internucleotide linkage cleaves, although higher-ordered RNA structure also contributes significantly to the rate of transesterification. Alkaline conditions favor specific base catalysis, in which the 2'-hydroxyl group is deprotonated by hydroxide to generate the more nucleophilic 2'-oxyanion group (Scheme 1, 1). In this process, the P–5'O bond of the phosphodiester linkage is cleaved upon formation of a new P–2'O bond to yield 2',3'-

**Scheme 1.** RNA Cleavage by Alkali-Promoted Transesterification<sup>a</sup>



<sup>a</sup> Structures 1 and 2 represent the 3',5'-phosphodiester linkage in the ground-state configuration and the pentacoordinate intermediate, respectively. Cleavage products carrying a 2',3'-cyclic phosphodiester terminus (3) and a 5'-hydroxyl terminus (4) are generated following nucleophilic attack by the 2' oxygen. B represents any of the four natural nucleotide base moieties. Dashed lines depict the continuation of the RNA chain via additional 3',5'-phosphodiester linkages or alternatively chain termination with hydrogen.

cyclic phosphate (3) and 5'-hydroxyl (4) termini. This cyclizing mechanism for RNA cleavage, which was first proposed and subsequently established by investigators during the early 1950s,<sup>2–6</sup> is the primary pathway for the uncatalyzed degradation of RNA polymers under typical cellular conditions.<sup>7</sup>

(2) Brown, D. M.; Todd, A. R. *J. Chem. Soc.* **1952**, 52–58.

(3) Bacher, J. E.; Kauzmann, W. *J. Am. Chem. Soc.* **1952**, 74, 3779–3786.

(4) Brown, D. M.; Todd, A. R. *J. Chem. Soc.* **1953**, 2040–2049.

(5) Lipkin, D.; Talbert, P. T.; Cohn, M. J. *J. Am. Chem. Soc.* **1954**, 76, 2871–2872.

(6) Brown, D. M.; Magrath, D. I.; Neilson, A. H.; Todd, A. R. *Nature* **1956**, 177, 1124–1125.

\* Address correspondence to this author. E-mail: ronald.breaker@yale.edu.

(1) Oivanen, M.; Kuusela, S.; Lönnberg, H. *Chem. Rev.* **1998**, 98, 961–990.

Although a tremendous quantity of data concerning this reaction has been generated over the years,<sup>1</sup> no systematic examination of the reaction kinetics has been reported for conditions that are of physiological relevance. Most importantly, we wanted to determine the kinetic parameters needed to more accurately estimate the rate of RNA transesterification under neutral pH conditions and ambient temperatures. A detailed understanding of the kinetics of RNA transesterification under high pH conditions makes possible a quantitative assessment of the chemical stability of RNA in various aqueous environments. In addition, these data provide kinetic parameters that would be useful for investigating the catalytic strategies used by RNA-cleaving enzymes and for designing RNA-cleaving enzymes, ribozymes, and nuclease mimics.<sup>8,9</sup>

## Results and Discussion

**RNA Substrates and the RNA Cleavage Assay System.** All internucleotide linkages within an RNA polymer can undergo cleavage by transesterification. Therefore, the kinetic analysis of RNA phosphoester cleavage in the context of large RNA polymers can be problematic. To examine the cleavage of an individual RNA phosphodiester, we synthesized five different 22-nucleotide DNAs that contain a single embedded RNA linkage located between nucleotides 12 and 13 (e.g., substrate S(ApG); Figure 1A). Degradative mechanisms that spontaneously act upon DNA, such as phosphoester hydrolysis,<sup>10</sup> oxidative cleavage,<sup>11</sup> and cleavage as a result of depurination,<sup>12</sup> are all at least several orders of magnitude slower than RNA transesterification under alkaline conditions. In this context, the cleavage of the lone RNA phosphodiester linkage can be assessed without complications resulting from unwanted cleavage of the flanking DNA phosphodiesters. As a result, these chimeric “embrRNA” substrates<sup>13</sup> provide an excellent alternative to the use of dinucleotides (e.g., see refs 7 and 14) for model compounds to study RNA degradation.

Higher-ordered nucleic acid structure could significantly affect the rate at which an internucleotide linkage undergoes cleavage by transesterification (see below). However, none of the five chimeric substrates used in this study are predicted<sup>15,16</sup> to form unimolecular or bimolecular secondary structures that could bias cleavage rates and therefore complicate data collection and analysis (the DNA mfold server can be accessed on the Internet at [www.ibc.wustl.edu/~zucker/dna/form1.cgi](http://www.ibc.wustl.edu/~zucker/dna/form1.cgi)). The reaction conditions most frequently used for data collection involved high pH or high temperature, both of which are expected to disfavor the formation of higher-ordered structures. Moreover, absorbance/temperature profiles conducted with the all-DNA version of S(ApG) at pH 7 and 10.6 indicate that no significant higher-ordered structures are formed that otherwise could bias the kinetics of RNA cleavage (data not shown).

Cleavage of a 5' <sup>32</sup>P-labeled version of the substrate S(ApG) at the RNA phosphodiester produces a single new <sup>32</sup>P-labeled product that corresponds to the 12-nucleotide 5'-cleavage

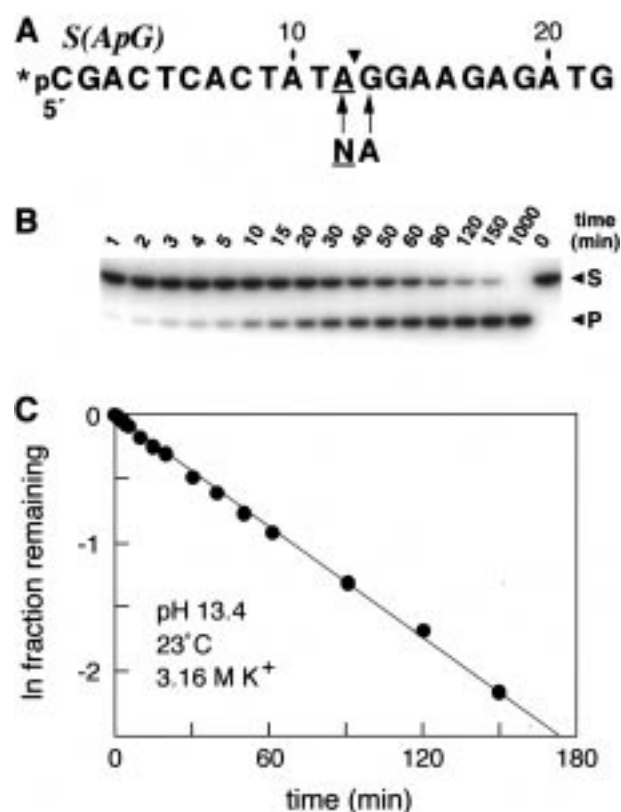


**Figure 1.** (A) Substrate oligonucleotides used for cleavage rate determinations. Each 22-nucleotide DNA contains a single ribonucleotide (underlined) that forms an embedded RNA phosphodiester linkage (triangle). Oligonucleotides are radiolabeled at the 5' terminus with <sup>32</sup>P (\*p). Nucleotide changes made to the parent sequence “S(ApG)” are identified by the arrows, where the sequence variations for each substrate are identified within the parentheses. (B) Representative autoradiogram of a typical separation of <sup>32</sup>P-labeled substrate (S) and <sup>32</sup>P-labeled product (P; 12-nucleotide 5'-cleavage fragment) made by denaturing 10% PAGE. Transesterification reactions with S(ApG) were conducted at pH 13.4 for the times indicated (see Experimental Section). The 5'-cleavage fragments carry heterogeneous termini consisting of 2',3'-cyclic phosphate, or the subsequent hydrolysis products 2' phosphate or 3' phosphate. Fragments with these different chemical configurations are not resolved with this analysis. (C) Representative plot depicting the decay of the RNA linkage as derived from the data in part B. For this plot, the negative slope of the line represents the rate constant for the reaction in 3.16 M KCl, pH 13.4 ( $k = 0.014 \text{ min}^{-1}$ ).

fragment as expected. Denaturing polyacrylamide gel electrophoresis is used to separate substrate and product molecules, and the resulting <sup>32</sup>P-labeled reaction products are imaged by autoradiography (Figure 1B). The relative amounts of each radiolabeled oligonucleotide were quantitated using a phosphor-based imaging system, which provides an extremely sensitive and accurate determination of product yields. A plot of the natural log of the fraction of substrate remaining at various incubation times forms a straight line over 3 half-lives when incubated at pH 13.4 (Figure 1C). This result indicates that the RNA transesterification reaction proceeds to near completion without variation in reaction kinetics. The negative slope of the resulting line provides the rate constant ( $k$ ) for RNA transesterification under the specific reaction conditions surveyed. This same approach was used to establish rate constants under all reaction conditions.

**Dependence of RNA Transesterification on pH.** The rate constant for cleavage of the substrate S(ApG) (Figure 1A) was determined at different pH values ranging between 8.75 and 14.5. At pH values below 12, 2-(cyclohexylamino)ethanesulfonic

(7) Järvinen, P.; Oivanen, M.; Lönnberg, H. *J. Org. Chem.* **1991**, 56, 5396–5401.

(8) Sigman, D. S.; Mazumder, A.; Perrin, D. M. *Chem. Rev.* **1993**, 93, 2295–2316.

(9) Trawick, B. N.; Daniher, A. T.; Bashkin, J. K. *Chem. Rev.* **1998**, 98, 939–960.

(10) Guthrie, J. P. *J. Am. Chem. Soc.* **1977**, 99, 3991–4001.

(11) Carmi, N.; Balkhi, S. A.; Breaker, R. R. *Proc. Natl. Acad. Sci. U.S.A.* **1998**, 95, 2233–2237.

(12) Lindahl, T. *Nature* **1993**, 362, 709–715.

(13) Jenkins, L. A.; Bashkin, J. K.; Autry, M. E. *J. Am. Chem. Soc.* **1996**, 118, 6822–6825.

(14) Koike, T.; Inoue, Y. *Chem. Lett.* **1972**, 569–572.



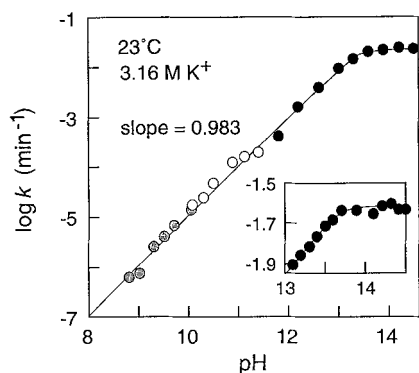


**Figure 2.** The pH dependence of the rate of S(ApG) RNA cleavage. Data were collected in reaction mixtures containing CHES (shaded circles) and CAPS (open circles) or in unbuffered (filled circles) reactions. Inset: High-resolution profile depicting the pH range that encompasses the transition from first-order to zero-order kinetics that occurs near the  $pK_a$  for the 2'-hydroxyl group. The apparent  $pK_a$  for the 2'-hydroxyl group of the ApG internucleotide linkage under these reaction conditions (3.16 M KCl, 23 °C) is  $\sim 13.1$ , as determined by the pH value that provides a value for  $k$  that is half-maximal ( $k_{\max} \sim 0.02 \text{ min}^{-1}$ ).

acid (CHES; pH 8.75 to 10) and 3-(cyclohexylamino)-1-propanesulfonic acid (CAPS; pH 10.25 to 11.75) were used to stabilize the hydroxide ion concentration. At pH values above 12, appropriate amounts of KOH were added to unbuffered reaction mixtures to establish the desired hydroxide ion concentration. No buffering agent was deemed necessary at these more alkaline pH conditions due to the high concentrations of hydroxide ions and the short incubation times that were needed to accurately establish rate constants for transesterification. In most instances, ionic strength was maintained constant in all reactions by supplementing each reaction mixture with KCl such that the total concentration of ionic potassium ( $K^+$ ) was 3.16 M. This concentration was chosen to normalize the amount of  $K^+$  delivered to each reaction with that delivered to the reaction at pH 14.5 in the form of KOH.

A linear relationship was revealed by plotting the logarithm of the rate constants for RNA transesterification between pH 9 and 13 (Figure 2). This correlation, which has been well documented by other investigators,<sup>7,14,17–20</sup> is due to the increasing fraction of 2'-oxyanion groups relative to 2'-hydroxyl groups that is produced under progressively higher hydroxide concentrations. Specific base catalysis generates a 10-fold increase in the number of reactive 2'-oxyanion groups for each unit increase in pH. This effect is reflected in Figure 2, where the line depicting the relationship between rate constant and pH maintains a slope of  $\sim 1$  below pH 13. This linear relationship holds until the pH of the reaction mixture approaches the  $pK_a$  of the 2'-hydroxyl group. When the pH matches the  $pK_a$ , half of the substrate oligonucleotide already carries the more powerful 2'-oxyanion, and further deprotonation at most can have a 2-fold effect on the rate constant for the reaction.

The line formed when plotting the rate constants obtained at pH values significantly greater than the  $pK_a$  for the 2'-hydroxyl

is predicted to have a slope of 0, as is seen with the data generated with S(ApG) near pH 14 (Figure 2, inset). The  $pK_a$  for the 2'-hydroxyl group can be inferred from the pH-dependent rate profile by determining the pH at which  $k$  is half its maximum value. Under these reaction conditions (3.16 M  $K^+$ , 23 °C), the maximum value for  $k$  or  $k_{\max}$  for S(ApG) equals  $\sim 0.022 \text{ min}^{-1}$ . The half-maximal rate constant or  $1/2 k_{\max}$  of  $\sim 0.011 \text{ min}^{-1}$  is obtained at pH of  $\sim 13.1$ , which establishes the apparent  $pK_a$  for the 2'-hydroxyl group of the labile internucleotide linkage of S(ApG) under these assay conditions. A  $pK_a$  value of 13.1 is consistent with the assumption that the  $pK_a$  of a lone 2'-hydroxyl group will be greater than  $\sim 12.4$ , which is the  $pK_a$  value observed<sup>21–24</sup> for a terminal hydroxyl of an RNA monomer when the vicinal 2' and 3' oxygen atoms remain unesterified.

Another critical parameter that can be established from these data is the rate constant for RNA transesterification at pH values that approximate physiological conditions. Unfortunately, experimental determination of rate constants below pH 9 becomes difficult due to the extremely slow rate of the reaction. Although long incubation times can be used to generate measurable amounts of cleavage product, the background rate of substrate cleavage due to radiolysis begins to contribute to the total observed rate for substrate cleavage, and interferes with data interpretation. Due to the linear nature of the pH-dependent rate profile, extrapolating the line toward acidic pH values should reveal the rates for RNA transesterification under biologically relevant conditions. This can be done with confidence through pH 6, assuming that pH only affects the protonation state of the 2'-hydroxyl group. With reaction conditions below pH 6, specific base catalysis (measured at elevated temperatures) becomes a minor mechanism relative to the competing mechanism of specific acid catalysis for RNA transesterification.<sup>1</sup> As a result, data extrapolation for specific base-catalyzed RNA cleavage under these acidic conditions also is problematic.

Equation  $a_1$  was derived from a simple slope-intercept form ( $y = mx + b$ ; see Experimental Section for details on the derivation of equations).

$$\log k = 0.983(\text{pH}) - 14.8 \quad (a_1)$$

This equation can be used to estimate the contribution that specific base catalysis makes toward the rate constant for RNA transesterification at any pH value below the  $pK_a$  of the 2'-hydroxyl group. A slope ( $m$ ) of 0.983 for the cleavage of S(ApG) was derived by plotting  $\log k$  versus pH (Figure 2). The y-intercept ( $b$ ) is determined as the y-intercept of the line formed by plotting pH-dependent rate constants for pH 9 to 13 using linear regression analysis. For ApG, a y-intercept of  $-14.8$   $\text{min}^{-1}$  is obtained at pH 0. The rate constant ( $y$ ) for RNA transesterification under different buffer conditions can be predicted by substituting different values for pH ( $x$ ).

By employing a more simplified equation (eq  $a_2$ ) with the above-described parameters, specific base-catalyzed cleavage of an ApG RNA linkage at 23 °C, pH 6.0, and in 3.16 M  $K^+$  is projected to proceed with an otherwise uncatalyzed rate constant ( $k_{\text{background}}$ ) of  $1.30 \times 10^{-9} \text{ min}^{-1}$ .

(15) Zuker, M. *Science* **1989**, *244*, 48–52.

(16) SantaLucia, J., Jr.; Allawi, H. T.; Seneviratne, P. A. *Biochemistry* **1996**, *35*, 3555–3562.

(17) Bock, R. M. *Methods Enzymol.* **1967**, *XIIA*, 218–221.

(18) Liu, X.; Reese, C. B. *Tetrahedron Lett.* **1995**, *36*, 3413–3416.

(19) Matsumoto, Y.; Komiya, M. *J. Chem. Soc., Chem. Commun.* **1990**, *15*, 1050–1051.

(20) Weinstein, L. B.; Earnshaw, D. J.; Cosstick, R.; Cech, T. R. *J. Am. Chem. Soc.* **1996**, *118*, 10341–10350.

(21) Levene, P. A.; Simms, H. S.; Bass, L. W. *J. Biol. Chem.* **1926**, *70*, 243–251.

(22) Izatt, R. M.; Hansen, L. D.; Rytting, J. H.; Christensen, J. J. *J. Am. Chem. Soc.* **1965**, *87*, 2760–2761.

(23) Izatt, R. M.; Rytting, J. H.; Hansen, L. D.; Christensen, J. J. *J. Am. Chem. Soc.* **1966**, *88*, 2641–2645.

(24) Birnbaum, G. I.; Giziewicz, J.; Huber, C. P.; Shugar, D. *J. Am. Chem. Soc.* **1976**, *98*, 4640–4644.

$$k = 10^{\{-14.8 + 0.983(\text{pH})\}} \quad (\text{a}_2)$$

At pH 6, both specific base catalysis and specific acid catalysis are near a minimum,<sup>1</sup> although cleavage by a depurination/ $\beta$ -elimination mechanism becomes increasingly significant.<sup>12</sup> However, the  $k_{\text{background}}$  value at pH 6 is of particular interest as it reflects the rate at which transesterification will occur under aqueous conditions that are presumed to be the safest for the long-term storage of RNA.

Equation  $\text{a}_2$  can be used to accurately predict the rate constants for RNA transesterification for pH values that range from 6 to values that approach the  $\text{pK}_a$  for the 2'-hydroxyl group. This equation, however, does not take into consideration that rate constants begin to plateau at pH values near and above the  $\text{pK}_a$ . Equation  $\text{a}_3$  is a modified form of  $\text{a}_2$  that can be used to

$$k = 10^{\{-14.80 - 0.983\log(K_a + [\text{H}^+])\}} \quad (\text{a}_3)$$

approximate the rate constants for pH values beginning at pH 6 and ranging beyond pH 13.1, which equals  $\text{pK}_a$  determined for the 2'-hydroxyl group of S(ApG). Values for the equilibrium constant  $K_a$  and  $[\text{H}^+]$  are the negative antilogarithms of the  $\text{pK}_a$  for the 2'-hydroxyl group and the pH of the reaction mixture, respectively.

**Power of 2'-Hydroxyl and 2'-Oxyanion Groups as Nucleophiles.** Nucleophilic attack by the 2' oxygen is the rate-limiting step for RNA transesterification under alkaline reaction conditions. Therefore, deprotonation of the 2'-hydroxyl group to yield the more nucleophilic 2' oxyanion directly influences the rate constant for transesterification. Beginning above pH 5, increasing the pH of the reaction mixture results in a corresponding linear increase in the logarithm of the rate constants for RNA transesterification.<sup>1</sup> This finding indicates that, even at pH values lower than 6, the deprotonated 2'-oxyanion form of the nucleophile dictates the rate constant observed for RNA cleavage.

Conversely, the data indicate that the protonated form of the nucleophile, the 2'-hydroxyl group, makes a negligible contribution to cleavage kinetics, even at pH values near 5. This is true despite the fact that at pH 5 the 2'-hydroxyl group is present in more than  $10^8$ -fold excess over the deprotonated form. Therefore, to play the dominant role in nucleophilic attack, the 2'-oxyanion group must be at least  $10^8$ -fold more powerful than its protonated counterpart. For comparison, the oxyanion group derived from methanol is  $\sim 10^6$ -fold more nucleophilic than its corresponding hydroxyl form when attacking a methyl iodide substrate in methanol solvent.<sup>25</sup> The  $\sim 100$ -fold discrepancy between these two values most likely reflects the influences that reaction parameters such as solvent and substrate types (among many other factors) have on the relative nucleophilic power of related attacking groups.<sup>26</sup>

**Dependence of  $\text{pK}_a$  on the Concentration of Potassium Ions.** Several reaction parameters other than pH also may affect the rate constants for RNA transesterification. We find that  $\text{K}^+$  concentration has a significant influence on the rate constants at a given pH. Specifically, increasing  $\text{K}^+$  concentrations yields progressively higher rate constants at pH values below 13 (data not shown). Unfortunately, we could not test whether the original  $k_{\text{max}}$  of  $0.022 \text{ min}^{-1}$  attained at  $3.16 \text{ M } [\text{K}^+]$  (Figure 2) changes with different concentrations of ionic potassium, because

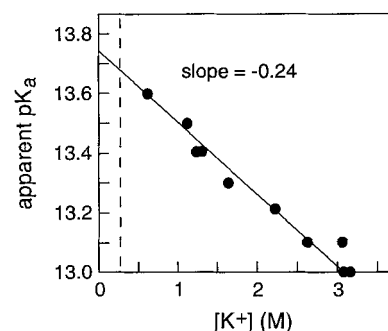


**Figure 3.** Influence of  $[\text{K}^+]$  on the apparent  $\text{pK}_a$  of the 2'-hydroxyl group at  $23^\circ\text{C}$ .

establishing pH values above the  $\text{pK}_a$  for the 2'-hydroxyl group using KOH would introduce excessive amounts of  $\text{K}^+$  into the reaction mixture. However, ionic potassium is expected to stabilize the deprotonated form of the 2'-hydroxyl group through ionic interactions, thereby lowering its  $\text{pK}_a$  and producing the increases in the observed rate constants. As a result, we speculate that the  $\text{pK}_a$ , and not the maximum rate constant, is most likely to be influenced by  $\text{K}^+$ .

If this assumption is correct, then observed increases in rate constants with increasing  $[\text{K}^+]$  exclusively reflect decreasing  $\text{pK}_a$  values for the 2'-hydroxyl group. Apparent  $\text{pK}_a$  values for the 2'-hydroxyl group at different concentrations of  $\text{K}^+$  were determined by establishing the pH values needed to achieve  $1/2 k_{\text{max}}$ . A comparison of apparent  $\text{pK}_a$  values versus  $[\text{K}^+]$  forms a linear plot with a slope of  $-0.24$  (Figure 3), which reflects the  $\sim 0.6$  unit shift in apparent  $\text{pK}_a$  over the concentration range of potassium used in this study. Although an apparent  $\text{pK}_a$  of 13.1 was established at high potassium concentration, a value of 13.7 is expected with potassium concentrations that approach those observed inside cells ( $\sim 0.25 \text{ M}$ ). This relationship holds even when taking into consideration the activity coefficients for KCl. At  $25^\circ\text{C}$  the activity coefficients that more accurately reflect the free concentration of  $\text{K}^+$  drop significantly between 0 and  $0.3 \text{ M}$ .<sup>27</sup> However, the coefficients decrease only slightly over the concentration range used in this study and, as a result, corrections for  $\text{K}^+$  activities were not made.

Rate constants can be calculated for RNA transesterification at different concentrations of  $\text{K}^+$  using eq b. The background rate constant ( $k_{\text{background}}$ ) used for this equation ( $1.30 \times 10^{-9} \text{ min}^{-1}$ ) is the value projected for RNA cleavage at pH 6.0 and  $23^\circ\text{C}$  in the presence of  $3.16 \text{ M } \text{K}^+$  using eq  $\text{a}_2$  (see above). The value for  $[\text{K}^+]$  should reflect the total molar concentration present under the reaction conditions of interest. Equation b begins with a  $k_{\text{background}}$  under the maximum  $[\text{K}^+]$  tested ( $3.16 \text{ M}$ ), and the additional factor adjusts this value for lower  $\text{K}^+$  concentrations.

$$k_{\text{projected}} = k_{\text{background}} \times 10^{\{-0.24(3.16 - [\text{K}^+])\}} \quad (\text{b})$$

**Transesterification Rates and the Concentration of Divalent Magnesium.** Cationic metals have profound effects on the folded structures and chemical stability of RNA molecules.<sup>28</sup> It has been known for many years that various divalent metal ions strongly promote RNA degradation by transesterification.<sup>29–32</sup>

(27) Weast, R. C. In *CRC Handbook of Chemistry and Physics*; CRC Press: Cleveland, OH, 1976; p D-153.

(28) Pan, T.; Long, D. M.; Uhlenbeck, O. C. In *The RNA World*; Gesteland, R. F., Atkins, J. F., Eds.; Cold Spring Harbor Laboratory Press: New York, 1993; pp 271–302.

(29) Butzow, J. J.; Eichorn, G. L. *Biopolymers* **1965**, 3, 95–107.

(30) Farkas, W. R. *Biochim. Biophys. Acta* **1968**, 155, 401–409.  
FDA-CBER-2022-1614-1035821

(25) Pearson, R. G.; Sobel, H.; Songstad, J. J. *Am. Chem. Soc.* **1968**, 90, 319–326.

(26) Pross, A. In *Theoretical and Physical Principles of Organic Reactivity*; John Wiley & Sons: New York, 1995; pp 232–234.

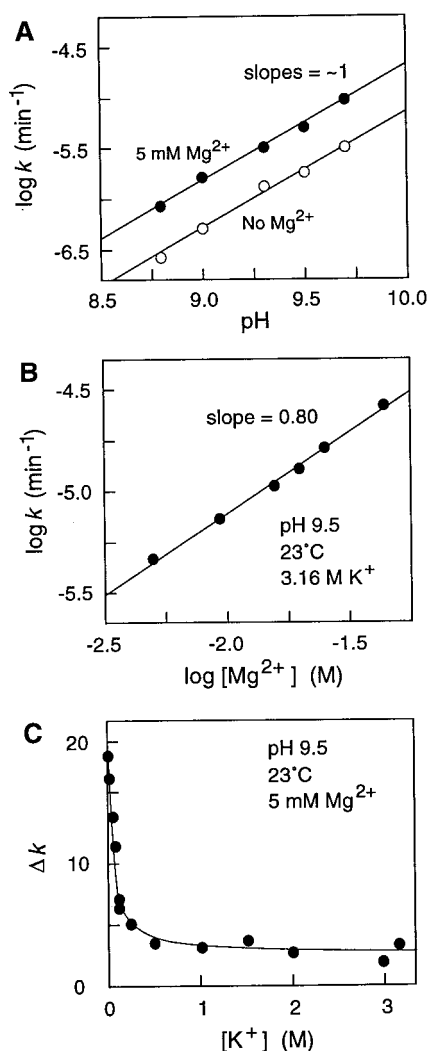


**Figure 4.** Influence of  $[Mg^{2+}]$  on the rate constant for RNA transesterification. Assay reactions for data depicted in part A were conducted at 23 °C in 3.16 M K<sup>+</sup> in the absence or presence of Mg<sup>2+</sup> as indicated, where the buffer (50 mM CHES) was adjusted to various pH values as shown. Similarly, reactions for data depicted in part B were conducted in 50 mM CHES (pH 9.5 at 23 °C) with various concentrations of MgCl<sub>2</sub>. The effect of  $[K^+]$  on Mg<sup>2+</sup>-promoted RNA cleavage (C) is expressed as the ratio ( $\Delta k$ ) of the rate constants in the presence of Mg<sup>2+</sup> versus the absence of Mg<sup>2+</sup>, at various concentrations of K<sup>+</sup>.

The catalytic roles of metal ions are diverse. For example, magnesium cations presumably could promote the cleavage of RNA by facilitating proton transfer or by serving as a Lewis acid catalyst.<sup>28,33</sup>

We examined the effects of divalent magnesium cations on the rate constant for RNA transesterification using concentrations of Mg<sup>2+</sup> that are of physiological relevance. At pH 9.5 and 3.16 M K<sup>+</sup>, the addition of divalent magnesium to 0.005 M induces an ~3-fold increase in rate constant over that observed in the absence of divalent metal ions. Moreover, this relationship holds for pH values ranging between 8.8 and 9.8 (Figure 4A). Assays under higher pH values were not attempted because higher hydroxide ion concentrations are expected to promote the formation of substantial amounts of insoluble

magnesium hydroxide complex,<sup>34</sup> and this would complicate the interpretation of any data that were derived under more alkaline conditions. As expected, increasing concentrations of MgCl<sub>2</sub> between 0.005 and 0.05 M bring about progressively faster rates of RNA cleavage. A plot of  $\log k$  versus  $\log [Mg^{2+}]$  at pH 9.5 reveals a linear relationship with a slope of 0.80 over the range of metal ion concentrations used (Figure 4B), reflecting the substantial impact that this particular divalent metal has on the rate of RNA transesterification.

In addition, we found that the concentration of K<sup>+</sup> also affects the rate enhancement caused by the addition of Mg<sup>2+</sup>. At concentrations of K<sup>+</sup> in excess of 0.5 M, the addition of 0.005 M Mg<sup>2+</sup> results in an ~3-fold increase in the rate constant. However, the influence of Mg<sup>2+</sup> increases sharply as the concentration of K<sup>+</sup> approaches zero (Figure 4C). The loss of Mg<sup>2+</sup>-promoted RNA cleavage at higher ionic strengths may be due to K<sup>+</sup>-mediated shielding of the negatively charged phosphates which may preclude the formation of RNA-Mg<sup>2+</sup> complexes. Mg<sup>2+</sup> may bind more strongly to the RNA phosphodiester backbone at low  $[K^+]$ , thereby accelerating transesterification by any of several mechanisms.

The effects of Mg<sup>2+</sup> that are made apparent in Figure 4 could be due to general base catalysis, general acid catalysis, catalysis by direct Lewis acid function, or in part may be due to the increase in ionic strength resulting from increasing  $[Mg^{2+}]$ . Regardless of the mechanism, the results described above indicate that rate constants for physiological pH conditions and concentrations of Mg<sup>2+</sup> can be predicted with reasonable accuracy. Equation c can be used to project the rate constants for RNA cleavage with Mg<sup>2+</sup> concentrations between 0.005 and 0.05 M and with concentrations of K<sup>+</sup> between 0.03 and 3.16 M. However, for reaction conditions with ion concentrations that are outside these ranges, this empirical equation may not provide accurate projections.

$$k_{\text{projected}} = k_{\text{background}} \times 69.3([Mg^{2+}]^{0.8}) \times 3.57([K^+]^{-0.419}) \quad (c)$$

The values for the first factor ( $k_{\text{background}}$ ) can be established using eq a between pH 6 and 13. The second factor represents the enhancement that Mg<sup>2+</sup> contributes to the overall rate constant as determined by the data in Figure 4B. The third factor reflects the influence that K<sup>+</sup> has on the RNA cleavage activity of Mg<sup>2+</sup>.

**Transesterification Rates and Temperature.** Temperature of the reaction mixture was found to have a substantial effect on the rate of RNA transesterification. In a reaction buffered with 50 mM CAPS (pH 10.7 at 23 °C), a linear trend between the rate constant and temperature is observed with progressively higher temperatures producing modest increases in the rate constant (Figure 5). However, the value for each rate constant must be corrected by considering the variation in pH that occurs when altering the temperature of the reaction mixture.<sup>35</sup> Specifically, the relevant  $pK_a$  of CAPS changes with increasing temperature ( $d\{pK_a\}/dT$ ) by a value of -0.032 unit per degree Celsius (see Experimental Section).

After correction for the changes in pH, the temperature-dependent variation in rate constants becomes much more pronounced. An increase in the rate constant of greater than 3 orders of magnitude is apparent between 4 and 50 °C after correcting the data for the inherent variation in pH (Figure 5A). A linear trend with a slope of 0.07 is observed for the influence

(31) Eichorn, G. L.; Tarien, E.; Butzow, J. J. *Biochemistry* **1971**, 10, 2014–2019.

(32) Zagórska, I.; Kuusela, S.; Lönnberg, H. *Nucleic Acids Res.* **1998**, 26, 3392–3396.

(33) Zhou, D.-M.; Taira, K. *Chem. Rev.* **1998**, 98, 991–1026.

(34) Dean, J. A., Ed. In *Lange's Handbook of Chemistry*, 13th ed.; McGraw-Hill: New York, 1985; pp 4–73.

(35) Ellis, K. J.; Morrison, J. F. *Methods Enzymol.* **1982**, 87, 405–426. FDA-CBER-2022-1614-1035822



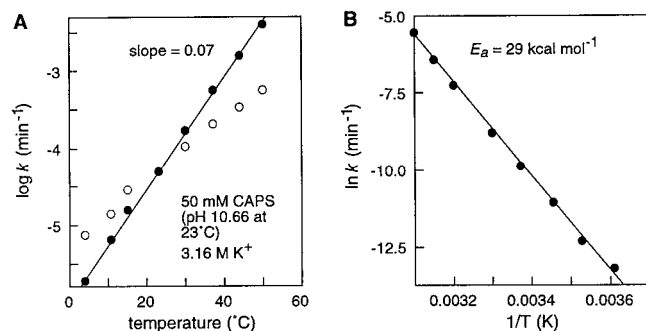


**Figure 5.** The effects of temperature on the rate constant for RNA transesterification. (A) Temperature dependence of rate constants plotted before (open circles) and after (filled circles) correction for pH variation. (B) Arrhenius plot of the corrected data depicted in part A.

of temperature on RNA transesterification in the presence of 3.16 M K<sup>+</sup>. The rate constant for a particular temperature can be calculated using eq d, where  $T_1$  is the temperature of interest,  $T_0$  is a temperature where the rate constant is known, and  $k_{T_0}$  is the value for the known rate constant.

$$k_{T_1} = k_{T_0} \times 10^{[0.07(T_1 - T_0)]} \quad (\text{d})$$

Cleavage of S(ApG) also produces a linear relationship between the reciprocal of the temperature and the natural logarithm of the rate constant (Figure 5B). This standard Arrhenius relationship indicates that the reaction kinetics are elementary and are not complicated by structure formation or other possible factors. The activation energy ( $E_a$ ) of the reaction is 29 kcal mol<sup>-1</sup>, compared with an  $E_a$  of 13.1 kcal mol<sup>-1</sup> determined for cleavage of RNA by a hammerhead ribozyme.<sup>36</sup>

**Transesterification Rate and Nucleotide Base Composition.** The precise structural orientation adopted by RNA linkages is known to be an important factor that influences the rate of cleavage by transesterification. It has been proposed<sup>37</sup> that the alignment of the attacking 2' oxygen must make its approach to the phosphate from the side opposite that of the 5'-oxygen leaving group for productive nucleophilic attack to occur. Indeed, this principle is consistent with the observed hydrolytic stability of duplex RNA, whose base stacking precludes the 3',5'-internucleotide linkages within its helical structure from adopting this permissive "in-line" orientation.<sup>38,39</sup> In contrast, the analogous 2',5'-internucleotide linkage becomes hypersensitive to strand scission when positioned within an otherwise normal RNA helix.<sup>38</sup> This latter observation is consistent with the hypothesis that a 2',5'-phosphodiester linkage favors an in-line conformation when embedded within a typical A-form RNA helix.

Likewise, it follows that base stacking within a single-stranded oligonucleotide that simulates the formation of an A-form helix<sup>40</sup> would also contribute to chemical stability. Therefore one would expect that nucleotide base composition, with its influence on the magnitude of single-stranded base stacking, may affect the rate at which an otherwise unconstrained RNA linkage undergoes cleavage by transesterification. Several early reports indicate that certain RNA sequences, particularly A-rich domains, are relatively resistant to alkali-promoted hydrolysis.<sup>14,41-44</sup>

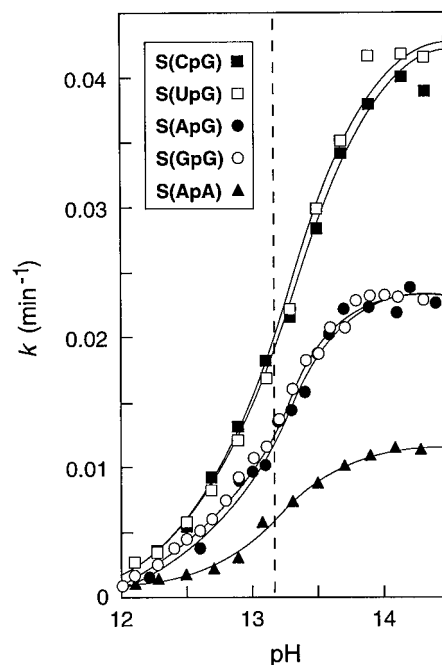


**Figure 6.** The effect of base composition on RNA transesterification. The dashed line demarks pH 13.1, a value that approximates the pK<sub>a</sub> for each of the internucleotide linkages examined. Reactions were conducted at 23 °C in 3.16 M K<sup>+</sup>.

For example, the dinucleotide ApA is estimated to cleave with a rate constant of  $3 \times 10^{-10}$  min<sup>-1</sup> at 50 °C and pH 6.0 in the absence of mono- or divalent metals.<sup>19</sup> Similarly, the dinucleotide pIpU (where I represents inosine) is projected to cleave with a rate constant of  $1 \times 10^{-10}$  under similar reaction conditions.<sup>20</sup> These rate constants are 5- to 10-fold lower than the rate constants projected for S(ApG) by the equations presented herein.

To investigate the effect that different nucleobase combinations may have on RNA phosphodiester stability, five representative linkages were assayed under alkaline conditions. A plot of the rate constants versus pH for substrate oligonucleotides containing the RNA internucleotide linkages CpG, UpG, ApG, GpG, and ApA is shown in Figure 6. Although the pK<sub>a</sub> values are essentially identical for each of the internucleotide linkages examined, the maximum rate constants derived for certain base compositions in fact do vary. S(ApA) is most resistant to specific base-catalyzed cleavage, as would be expected from data reported previously. However, our data indicate that the ApA linkage displays only a modest ~2-fold slower rate of transesterification ( $k = 0.01$  min<sup>-1</sup>) compared to the linkages ApG and GpG. Moreover, the substrates that display the fastest rate constants, S(CpG) and S(UpG), were only 4-fold more labile than that observed for S(ApA) ( $k = 0.04$  min<sup>-1</sup>). Although the differences in stability due to nucleotide base identities are relatively small, these differences would be sufficient to yield residual A-rich oligonucleotides upon alkaline digest as observed by previous investigators.<sup>41-44</sup>

The modest stabilization of ApA RNA linkages under alkaline conditions can in part be rationalized by the fact that single strands of homoadenylic acid polymers in particular adopt

(36) Uhlenbeck, O. C. *Nature* **1987**, 328, 596-600.

(37) Usher, D. A. *Proc. Natl. Acad. Sci. U.S.A.* **1969**, 62, 661-667.

(38) Usher, D. A.; McHale, A. H. *Proc. Natl. Acad. Sci. U.S.A.* **1976**, 73, 1149-1153.

(39) Reynolds, M. A., et al. *Nucleic Acids Res.* **1996**, 24, 760-765.

(40) Sanger, W. In *Principles of Nucleic Acid Structure*; Springer-Verlag: New York, 1984; pp 220-241, 302-304.

(41) Smith, K. C.; Allen, F. W. *Biochim. Biophys. Acta* **1953**, 75, 2131-2133.

(42) Potter, J. L.; Dounce, A. L. *J. Am. Chem. Soc.* **1956**, 78, 3078-3082.

(43) Lane, B. G.; Butler, G. C. *Biochim. Biophys. Acta* **1958**, 33, 281-283.

(44) Bock, R. M. *Methods Enzymol.* **1967**, XIIA, 218-221.

relatively stable A-form-like structures. As in the context of an A-form duplex, the internucleotide linkages that bridge the stacked bases within these single-stranded structures adopt a configuration that inherently disfavors in-line attack. Moreover, the adenine base moiety is not susceptible to deprotonation under alkaline conditions as are guanosine and uridine. Deprotonation of the base moiety would create a charge-repulsion effect that is expected to denature the helical structure of adjacent G and U residues,<sup>44</sup> thereby increasing the frequency in which the adjoining phosphodiester linkages sample the in-line orientation. The finding that the  $pK_a$  values for each dinucleotide combination tested are identical, coupled with the observation that the maximum rate constants observed for these substrates differ, supports a mechanism wherein each internucleotide linkage exists for different lengths of time in an in-line configuration. Moreover, the structural requirements invoked here are consistent with the finding that RNA linkages with a propensity to adopt an in-line configuration are more susceptible to spontaneous cleavage by transesterification.<sup>45</sup>

All the dinucleotide combinations examined in this study are predicted to display rate constants for cleavage at pH 6.0 and low ionic strength that range between  $10^{-9}$  and  $10^{-10} \text{ min}^{-1}$ . These predicted values closely approximate the rate constants reported previously for cleavage of similar RNA dinucleotides.<sup>19</sup> In addition, the maximum rate constant obtained for the specific base-catalyzed cleavage of the dinucleotide pIpU<sup>20</sup> is only 2-fold less ( $k = 0.005 \text{ min}^{-1}$ ) than that observed by us for ApA. Although different substrate forms and methods were used to establish these rate constants, their similarity to our data supports the validity of projecting rate constants using the current set of kinetic parameters. Moreover, it is apparent through our studies of S(ApG) that the ApG RNA linkage has kinetics for transesterification that are typical for an RNA linkage.

Under these same conditions, however, the dinucleotide UpA has been demonstrated<sup>46</sup> to cleave with a rate constant of  $3 \times 10^{-7} \text{ min}^{-1}$ , which is  $\sim 100$ -fold greater than that projected for the dinucleotide ApA. Moreover, many dinucleotides of the form UpA or CpA in the context of natural RNA polymers undergo cleavage via transesterification with rates that far exceed other internucleotide linkages.<sup>47,48</sup> Either a substantial shift in the  $pK_a$  of the 2'-hydroxyl group or a dramatic increase in the "in-line" nature of the linkage may be responsible for the unusual cleavage rates observed for these dinucleotides. Additional experimentation is currently underway to examine the underlying cleavage mechanism of these unique dinucleotides.

**A General Equation for Estimating Rate Constants for RNA Transesterification.** A variety of factors may affect the accuracy of rate constants that are derived from the equations described above. Of foremost importance is the accuracy of the data from the rate constants and trends used to establish each equation. We find that the assay system used in this study is simple to implement, is free of complications, and yields highly reproducible kinetic parameters and trends. In certain cases (e.g., pH and  $K^+$ ) the mechanism responsible for a condition-dependent change in rate constant may be rationalized. However, the mechanisms that mediate the effects of  $Mg^{2+}$  and temperature are most likely complex. Also of significant importance is the structural configuration of the RNA linkage of interest. Although the ApG RNA linkage displays average reaction

**Table 1.** Projected versus Measured Rate Constants<sup>a</sup>

pH	temp (°C)	[K <sup>+</sup> ] (M)	[Mg <sup>2+</sup> ] (M)	reaction conditions		
				$k \text{ (min}^{-1}\text{)}$		accuracy
				projected	measured	
9.4	40	0.26	0.005	$5.1 \times 10^{-5}$	$5.5 \times 10^{-5}$	-0.1
9.4	40	1.1	0.05	$2.7 \times 10^{-4}$	$8.6 \times 10^{-4}$	-2.1
9.5	23	0.03	0	$6.3 \times 10^{-7}$	$5.2 \times 10^{-7}$	0.2
9.5	23	0.15	0	$6.8 \times 10^{-7}$	$1.1 \times 10^{-6}$	-0.6
9.5	23	0.15	0	$6.8 \times 10^{-7}$	$5.9 \times 10^{-7}$	0.1
9.5	23	0.25	0	$7.1 \times 10^{-7}$	$9.7 \times 10^{-7}$	-0.4
9.5	23	0.5	0	$8.1 \times 10^{-7}$	$1.1 \times 10^{-6}$	-0.3
9.5	23	1	0	$1.0 \times 10^{-6}$	$1.3 \times 10^{-6}$	-0.2
9.5	23	1.5	0	$1.4 \times 10^{-6}$	$9.4 \times 10^{-7}$	0.3
9.5	23	2	0	$1.8 \times 10^{-6}$	$1.4 \times 10^{-6}$	0.2
9.5	23	3	0	$3.2 \times 10^{-6}$	$2.1 \times 10^{-6}$	0.3
9.5	23	0.03	0.005	$9.8 \times 10^{-6}$	$1.1 \times 10^{-5}$	-0.1
9.5	23	1	0.005	$3.8 \times 10^{-6}$	$3.2 \times 10^{-6}$	0.2
9.5	23	2	0.005	$4.9 \times 10^{-6}$	$2.2 \times 10^{-6}$	0.6
9.5	23	3	0.005	$7.1 \times 10^{-6}$	$4.7 \times 10^{-6}$	0.3
9.5	37	0.26	0.005	$3.9 \times 10^{-5}$	$1.1 \times 10^{-4}$	-1.9
9.6	37	1	0.05	$2.6 \times 10^{-4}$	$1.1 \times 10^{-3}$	-3.2
9.7	37	0.25	0.005	$6.1 \times 10^{-5}$	$6.2 \times 10^{-5}$	-0.0
10.0	23	1	0.05	$7.5 \times 10^{-5}$	$2.3 \times 10^{-4}$	-2.0
10.0	23	2	0.01	$2.7 \times 10^{-5}$	$1.2 \times 10^{-4}$	-3.5
10.1	23	0.25	0.005	$1.8 \times 10^{-5}$	$3.5 \times 10^{-5}$	-1.0
10.1	50	1.1	0	$3.7 \times 10^{-4}$	$3.3 \times 10^{-4}$	0.1
10.5	40	1.1	0	$1.5 \times 10^{-4}$	$1.4 \times 10^{-4}$	0.1
10.6	4	1	0.05	$1.4 \times 10^{-5}$	$3.8 \times 10^{-5}$	-1.8
10.6	4	2	0.01	$4.9 \times 10^{-6}$	$1.2 \times 10^{-5}$	-1.5
10.7	4	0.25	0.005	$3.3 \times 10^{-6}$	$3.6 \times 10^{-6}$	-0.1
12.0	23	0.01	0	$1.7 \times 10^{-4}$	$6.0 \times 10^{-5}$	0.6
12.5	23	0.03	0	$4.5 \times 10^{-4}$	$1.8 \times 10^{-4}$	0.6
13.0	23	0.1	0	$1.0 \times 10^{-3}$	$1.1 \times 10^{-3}$	-0.1

<sup>a</sup> Accuracy between projected and measured rate constants is defined as  $(k_{\text{projected}} - k_{\text{measured}})/k_{\text{projected}}$ .

kinetics, other dinucleotides such as UpA and CpA cleave much faster when examined in isolation. In fact, the rates of cleavage of any internucleotide linkage, regardless of nucleotide base composition, conceivably could be enhanced or diminished by higher-ordered RNA structures.

Despite these uncertainties, a predictive equation that simultaneously accounts for each of the reaction variables described above would be of considerable value for estimating rate constants for an "average" internucleotide linkage. Equation e

$$k_{\text{projected}} = k_{\text{background}} \times 10^{\{0.983(\text{pH}-6)\}} \times 10^{\{-0.24(3.16-[K^+])\}} \times 69.3[Mg^{2+}]^{0.80} \times 3.57[K^+]^{-0.419} \times 10^{\{0.07(T_1-23)\}} \quad (\text{e})$$

integrates each of the reaction parameters into a single expression, thereby allowing the estimation of cleavage rate constants when two or more of these variables are altered simultaneously. Here again,  $k_{\text{background}} = 1.30 \times 10^{-9} \text{ min}^{-1}$  at 23 °C, pH 6.0, and 3.16 M  $K^+$ . The next factor is a variation of eq a<sub>2</sub> that reflects the change in the rate constant relative to pH 6. The remaining elements of the equation are assembled from eqs b–d, respectively. The background rate constant has been estimated for a temperature ( $T_0$ ) of 23 °C. Since eq e integrates factors from eq c, the resulting general equation is expected to be accurate only for reaction conditions with the above-specified range of ion concentrations.

As a test of the utility of this equation, we examined the rate constants for cleavage of S(ApG) under conditions where several reaction parameters were varied simultaneously (Table 1). In each case, the rate constants generated using eq e predict the experimentally determined rate constants to within 5-fold. The accuracy for these approximations holds for different reaction mixtures that produce rate constants ranging over 4 orders of

(45) Soukup, G. A.; Breaker, R. R. Submitted for publication.

(46) Thompson, J. E.; Kutateladze, T. G.; Schuster, M. C.; Venegas, F. D.; Messmore, J. M.; Raines, R. T. *Bioorg. Chem.* **1995**, *23*, 471–481.

(47) Kierzek, R. *Nucleic Acids Res.* **1992**, *20*, 5079–5084.

(48) Williams, K. P.; Ciafré, Tocchi-Valentini, G. P. *EMBO J.* **1995**, *14*, 4551–4557.

magnitude, and where as many as four reaction conditions are altered simultaneously.

The set of empirical equations derived in this study is expected to be useful for the estimation of RNA cleavage rates under physiological conditions, and under conditions that are likely to be used for the manipulation and study of nucleic acids. Establishing these and other kinetic values will provide a valuable set of parameters that could be employed in efforts to make an accurate accounting for the rate enhancements of RNA-cleaving catalysts and enzymes. For example, one can estimate the rate constants at which RNA will undergo degradation via transesterification under representative physiological conditions (e.g., 37 °C, pH 7.4, 0.25 M K<sup>+</sup>, and 0.005 M Mg<sup>2+</sup>). Using eq e, the background reaction for S(ApG) under these conditions is projected to be  $1.4 \times 10^{-7} \text{ min}^{-1}$ . This value approximates the experimentally derived values obtained under similar reaction conditions.<sup>49,50</sup> Interestingly, the rate constant for RNA transesterification under representative physiological conditions is  $\sim 100\,000$ -fold greater than the estimated rate constant of  $\sim 10^{-12} \text{ min}^{-1}$  for the hydrolysis of DNA under similar reaction conditions,<sup>51</sup> reflecting the substantial difference in chemical stability between these two nearly identical polymers.

Equation e can also be used to define the challenges that are encountered by organisms that live in extreme environments or that may generate extreme conditions in vivo. For example, the rate constant for the uncatalyzed cleavage of individual internucleotide linkages within an unstructured RNA under conditions such as those experienced by thermophilic organisms (e.g., 100 °C, pH 7.4, 0.25 M K<sup>+</sup>, and 0.005 M Mg<sup>2+</sup>) is predicted by eq e to be  $\sim 1 \times 10^{-2} \text{ min}^{-1}$ . Therefore, RNAs of similar size are expected to spontaneously cleave nearly 100 000-fold faster in thermophilic organisms than in most mesophilic organisms. For comparison, the half-life for RNAs that are 1000 nucleotides (or larger) is expected to be  $\sim 1$  min or less due to the increased chemical instability of RNA at such high temperatures. Even smaller cellular RNAs such as tRNA would have a half-life of only  $\sim 10$  min at 100 °C, although the highly structured nature of these molecules should offer some protection from spontaneous strand cleavage. The inherent decrease in the chemical stability of RNA under more extreme conditions poses a serious challenge for thermophilic organisms, which most likely must use additional biochemical strategies to stabilize cellular RNAs against rapid spontaneous degradation.

## Conclusions

The process of general base catalysis is one of several catalytic strategies used by RNA-cleaving proteins such as bovine pancreatic ribonuclease A.<sup>52</sup> General base catalysis is manifest in this enzyme through histidine 12, which by deprotonation activates the 2'-hydroxyl group for nucleophilic attack. Apart from the source of the base catalyst, this mechanism is identical to that for specific base catalysis as examined in this study. As a result, we can use the kinetic parameters established herein to estimate the maximum rate enhancement for RNA transesterification that can be achieved either by specific base catalysis or by general base catalysis. The overall rate enhancement for specific base catalysis of RNA transesterification can be determined at different pH values by calculating the difference in the magnitude of  $k$  observed at a

given pH and the maximum  $k$  that can be achieved with total deprotonation of the 2'-hydroxyl group. For example, the estimated rate constant for the uncatalyzed cleavage of S(ApG) at 23 °C, pH 7 in 0.25 M K<sup>+</sup>, and 0.005 M Mg<sup>2+</sup> is  $\sim 1 \times 10^{-8} \text{ min}^{-1}$ . Our data also indicate that a catalyst or an enzyme that makes use of general base catalysis alone cannot exceed the experimentally derived  $k_{\text{max}}$  of  $0.022 \text{ min}^{-1}$  for the substrate S(ApG) that was measured under strong alkaline conditions (Figures 2 and 6). Therefore the maximum rate enhancement that can be achieved by a catalyst or enzyme that is restricted to general base catalysis under these conditions is  $\sim 2$  million fold. In contrast, a catalyst that fully exploits general base catalysis at pH 6 ( $k_{\text{background}} = \sim 1 \times 10^{-9} \text{ min}^{-1}$ ) conceivably could function with a 10-fold greater range, thereby displaying a maximum rate enhancement of  $\sim 20$  million fold.

Assuming that the changes in reaction parameters from our standard conditions have only a minor effect on the maximum rate constant of  $0.022 \text{ min}^{-1}$ , then this value should approximate the maximum rate constant that can be achieved by an RNA-cleaving enzyme that makes exclusive use of general base catalyst. By comparison, ribonuclease A<sup>53</sup> and the hammerhead ribozyme<sup>54</sup> display rate constants of  $\sim 1 \times 10^5$  and  $\sim 1 \text{ min}^{-1}$ , respectively, when operating under similar reaction conditions. Therefore, both of these natural RNA-cleaving enzymes must make use of alternative or additional catalytic strategies that allow them to exceed the maximum rate constant that is permitted by general base catalysis alone.<sup>55</sup>

## Experimental Section

**Synthesis of Embedded RNA Substrates.** Chimeric DNA/RNA substrates each were generated by reverse transcriptase (RT) extension of radiolabeled 12-nucleotide primer 5'-CGACTCACTAT(rN<sub>1</sub>), where (rN<sub>1</sub>) represents one of the four standard ribonucleotide monomers. Ribonucleotide-terminated primers were synthesized by solid-phase methods (Keck Biotechnology Resource Laboratory, Yale University) using the appropriate ribonucleotide-modified solid support. Purified 5'-<sup>32</sup>P-labeled primers were combined with the appropriate 28-nucleotide template DNA 5'-CATCTCTTC(N<sub>2</sub>')(N<sub>1</sub>')ATAGTGAGTCGTATTAG, where (N<sub>1</sub>') is complementary to the ribonucleotide base (N<sub>1</sub>) of the corresponding primer, and (N<sub>2</sub>') is varied to establish the identity of the base that flanks the 3' side of the RNA internucleotide linkage. To prepare the substrates used in this study, (N<sub>1</sub>) was set to G, A, U, or C; (N<sub>1</sub>') was set to C, T, A, or G, respectively; and (N<sub>2</sub>') was set to C or T (see Figure 1). RT-mediated extensions each were conducted in 100  $\mu\text{L}$  reaction mixtures containing 5  $\mu\text{M}$  primer, 10  $\mu\text{M}$  corresponding template, 0.4 mM each dNTP, and 600 U SuperScript II RT (Gibco BRL) and incubated for 1 to 2 h at 37 °C in the buffer solution supplied by the manufacturer. The extra nucleotides at the 3' terminus of each template facilitated efficient separation of the resulting 22-nucleotide substrates by denaturing 20% polyacrylamide gel electrophoresis (PAGE). Radiolabeled substrates were isolated from the gel by crush/soak elution and concentrated by precipitation with ethanol. The resulting precipitate was resuspended in deionized water and stored at  $-20$  °C until use.

**Kinetic Assays.** For typical assays, 5'-<sup>32</sup>P-labeled substrates ( $\sim 5$  nM) were incubated for various times in a reaction buffer containing a final concentration of 3.16 M K<sup>+</sup> and supplemented with 50 mM CHES or CAPS buffer as indicated. The pH for each reaction was set using buffer solutions with predetermined pH values, or by adding KOH to provide the specific concentration of hydroxide required to establish a given pH. Temperatures were maintained at 23 °C unless otherwise indicated. Each reaction aliquot was quenched by dilution into Tris-HCl buffer (pH 7.0 at 23 °C). Samples were further diluted (2-fold) by

(49) Breaker, R. R.; Joyce, G. F. *Chem. Biol.* **1995**, *2*, 655–660.

(50) Chapman, W. H.; Breslow, R. *J. Am. Chem. Soc.* **1995**, *117*, 5462–5469.

(51) Radzicka, A.; Wolfenden, R. *Science* **1995**, *267*, 90–93.

(52) Walsh, C. In *Enzymatic Reaction Mechanisms*; W. H. Freeman: New York, 1979; pp 199–207.

(53) DelCardayré, S. B.; Raines, R. T. *Biochemistry* **1994**, *33*, 15813–15828.

(54) Fedor, M. J.; Uhlenbeck, O. C. *Biochemistry* **1992**, *31*, 12042–12054.

(55) Li, Y.; Soukup, G. A.; Roth, A.; Breaker, R. R. In preparation. FDA-CBER-2022-1614-1035825



the addition of a gel loading buffer to give a final mixture containing 44 mM Tris–borate (pH 8.5), 3.5 M urea, 10% sucrose (w/v), and 0.0025% (w/v) each of bromophenol blue and xylene cyanol in addition to the original constituents of the reaction mixture. The samples were held on ice until gel loading. Reaction products were separated by 10% denaturing PAGE, and product yields were determined by imaging and quantitating the resulting bands using a PhosphorImager and Image-QuaNT software (Molecular Dynamics).

The influence of  $[K^+]$  on the apparent  $pK_a$  of the 2'-hydroxyl group was quantified by establishing the rate constants derived using different  $K^+$  concentrations under various pH conditions ranging from 12.9 to 13.6. For example, the  $[K^+]$  concentration required to achieve  $1/2k_{\max}$  at pH 13.5 was determined by supplementing the 0.316 M  $K^+$  derived from KOH with 0 to 2 M KCl. The rate constants obtained at different total concentrations of  $K^+$  were then compared with the expected value for  $1/2k_{\max}$  of  $0.01 \text{ min}^{-1}$ , which was obtained from the data depicted in Figures 2 and 6.

The effects of temperature variation on RNA transesterification were determined with cleavage assays similar to those described above. Substrate was combined with 50 mM CAPS (pH 10.66 at 23 °C) and 3.16 M  $K^+$  and incubated at various temperatures that were maintained by a thermocycler (DeltaCycler II, EriComp). The pH values for each reaction were estimated by subtracting or adding 0.032 pH units for each degree of variance from 23 °C.<sup>35</sup> The accuracy of this correction was examined by experimentally determining the pH of a 50 mM solution of CAPS (pH 10.66 at 23 °C) at several different temperatures. For example, the pH values for this solution at 4 and 50 °C are predicted to be 11.27 and 9.80, respectively. The pH values for these solutions were found to be 11.34 and 9.93, respectively, as measured using a standard Ag/AgCl ATC (automatic temperature compensation) electrode (Fisher) with an Accumet Basic pH meter.

**Determination of Rate Constants.** In many instances, rate constants were determined under various reaction conditions by first plotting the natural log of the fraction of substrate remaining uncleaved at various incubation times (e.g., Figure 1C). The negative slope of the resulting line, generated by a least-squares fit to the data, reflects the rate constant for RNA cleavage by transesterification. Data reported are representative of at least two separate experiments where the values for each repetition differed by less than 50%. When numerous rate constants were to be established (e.g., Figure 6), at least two time points taken during the early phase of the reaction (less than 10% cleaved) were examined. Plotting the fraction of substrate cleaved versus reaction time generates a slope that represents the initial velocity of the reaction. Cleavage reactions were shown to proceed to completion (Figure 1B), therefore no corrections for cleavage-resistant substrate were necessary.

**Equation Derivations.** Equations  $a_1$  and  $a_2$  were derived from the slope-intercept form equation using data derived from Figure 2. Equation  $a_3$  was derived from the Henderson–Hasselbalch equation that relates the protonation state of an acid to its  $pK_a$  and the pH of the medium:

$$pH = pK_a + \log([A^-]/[HA])$$

Therefore, the logarithm of the rate constant ( $k$ ) for RNA cleavage is dependent on the protonation state of the 2'-hydroxyl group according to the following equation:

$$\log k = -14.8 - 0.983\{\log(K_a + [H^+])\}$$

Further simplification yields eq  $a_3$  as given in the text.

The effect of  $[K^+]$  on the rate constant for RNA cleavage is reflected by eq b. This equation adjusts the value of a basal rate constant determined in the absence of  $K^+$  ( $k_{\text{background}}$ ) by a factor that reflects the influence of  $[K^+]$ . From Figure 3, we find that the apparent  $pK_a$  decreases with increasing concentration of  $K^+$  according to the following formula:

$$\text{apparent } pK_a = 13.1 + \{-0.24(3.16 - [K^+])\}$$

Here, the value 13.1 was derived experimentally from the data in Figure 3. The change in  $k_{\text{background}}$  relative to the change in  $pK_a$  of the 2'-hydroxyl group is then represented by the following equation:

$$\log k_{\text{projected}} = \log k_{\text{background}} + \{-0.24(3.16 - [K^+])\}$$

Further simplification yields eq b as given in the text.

The effect of  $Mg^{2+}$  and its modulation by  $K^+$  on  $k_{\text{background}}$  are encompassed by eq c. The impact of different concentrations of  $Mg^{2+}$  can be predicted by the following equation:

$$\log k = 0.8 \log[Mg^{2+}]$$

This linear relationship has only been determined between 0.005 and 0.05 M  $Mg^{2+}$  (Figure 4B). As a result, the equation derived from these data may only be valid over this same concentration of divalent ions. We have chosen 0.005 M  $Mg^{2+}$  as a reference point, giving the modified equation shown below:

$$k_{\text{projected}} = k_{\text{background}}([Mg^{2+}]/0.005)^{0.8}$$

This equation further simplifies to give the first two factors of eq c.

The effect of  $[K^+]$  on the catalytic activity of  $Mg^{2+}$  is represented by the following equation which was derived by a nonlinear fit to the data in Figure 4C:

$$\Delta k = 3.57[K^+]^{-0.419}$$

This equation is incorporated into eq c as the third factor without further modification.

The linear effect of temperature on the logarithm of the rate constant is represented by the following equation where  $T_0$  and  $T_1$  are the initial and final temperatures (°C), respectively, and  $k_{T_0}$  is an established rate constant at  $T_0$ :

$$\log k_{T_1} = (\log k_{T_0})\{0.07(T_1 - T_0)\}$$

Further simplification yields eq d as given in the text.

Equation e successively combines the factors that form eq  $a_2$  and eqs b–d to give an expression that can be used to approximate the rate constant for RNA cleavage under a variety of reaction conditions.

**Acknowledgment.** We thank members of the Breaker laboratory for comments on the manuscript and Dr. E. J. Behrman for helpful suggestions. This work was supported by a postdoctoral fellowship from the Medical Research Council of Canada to Y.L. and by a research grant from Ribozyme Pharmaceuticals, Inc.

JA990592P